SOLUTION MINING RESEARCH INSTITUTE
105 Apple Valley Circle
Clarks Summit, PA 18411, USA

Telephone: +1 570-585-8092
Fax: +1 505-585-8091
www.solutionmining.org

Technical Conference Paper

# MULTI–CYCLE GAS STORAGE IN SALT CAVERNS

Mehdi Karimi–Jafari, Geostock, Rueil, France
Nicolas Gatelier, Geostock, Rueil, France

Benoît Brouard, Brouard Consulting, Paris, France

Pierre Bérest, Ecole Polytechnique, Palaiseau, France
Hippolyte Djizanne, Ecole Polytechnique, Palaiseau, France

SMRI Fall 2011 Technical Conference
3–4 October 2011
York, United Kingdom

Solution Mining Research Institute Fall 2011 Technical Conference
York, United Kingdom, 3–4 October 2011

# MULTI–CYCLE GAS STORAGE IN SALT CAVERNS

M. Karimi–Jafari, N. Gatelier, B. Brouard, P. Bérest, H. Djizanne

**Abstract**

Today there is a growing demand from the operators of gas storage in salt cavern for quick cycling operation mode. Gas price fluctuation and trading issues make gas operators more interested in daily micro–cycle service than purely seasonal storage. Thus the main question is to what extent such a quick cycling operation is permitted from a thermo–mechanical point of view to ensure the cavern stability and integrity.

In this paper, some thermo–mechanical simulations of the salt cavern behaviour under different gas operation scenarios are discussed. Two main scenarios are compared: a purely seasonal storage versus a combined seasonal micro–cycling operation. The studied seasonal micro–cycling operation mode consists in weekly/daily pressure variation super–imposed on the purely seasonal storage.

The gas thermodynamic simulations are performed to optimize envelope of the seasonal micro–cycling operation taking into account the geotechnical and operational constraints.

Thermo–mechanical computations are performed to predict the stress and strain state in the rock salt. The cavern stability is verified applying the conventional criteria: no–tension and limited dilation in the rock salt.

Numerical simulations show that the seasonal micro–cycling scenario gives more favourable results than the purely seasonal one. The seasonal micro–cycling, fulfilling mechanical stability issues, provides higher cavern performance and larger working gas.

**Key words:** Gas Storage Caverns, Multi–cycling, Computer Modeling, Rock Mechanics, Gas Operation Performance

## Introduction

In contrast with traditional low–turn storages, such as depleted reservoirs and aquifers, salt caverns offer greater operational flexibility, allow higher deliverability and adjustment of storage capacity to growing gas price volatility.

However high deliverability of salt caverns is limited by several operational and geotechnical constraints. Operational constraints are related to the maximum operational gas flow rate originating from the risks of production tube erosion or tubing blockage due to hydrate formation. In some cases, the gas flow rate is limited by the head–pressure losses in the connection to the transmission network. Geotechnical constraints are the rock mechanical criteria for cavern stability and tightness.

In most cases, gas storages experiences seasonal variations (gas is injected during summer and withdrawn during winter). High deliverability multi–cycling operations consist of two different modes which can be defined as follows:

- multiple macro–cycling during which the total working gas is turned over several times per year.
- seasonal micro–cycling which consists of weekly/daily pressure variations (micro–cycling) superimposed on the purely seasonal variations.

The first mode (multiple macro–cycling) may imply very high pressure variations over withdrawal/injection periods. In the second mode (seasonal micro–cycling), cavern pressure variation is relatively small when compared to the overall gas pressure range ( $P_{\max} - P_{\min}$ ).

In this paper, seasonal micro-cycling gas operation is studied from a thermo–mechanical point of view and compared with a purely seasonal scenario.

**Operational constraints**

Generally, operational constraints on gas flow rate are related to the following issues:

- wellbore performance (gas pressure loss)
- production tubing erosion and noising
- Cavern performance (cavern pressure/temperature drop)
- Hydrate formation at wellhead (low withdrawal temperature).

Wellbore performance depends on gas completion. Larger the string diameter, smaller the pressure losses between the bottom and top of the well. API 14 recommends limiting the gas velocity below the following value to avoid any risk of tube erosion:

$$v_{\max} = 0.064 \cdot C_E \sqrt{\frac{T}{GP}} \tag{1}$$

where

- $T$ is gas temperature in K,
- $G$ is gas density with respect to air,
- $P$ is gas pressure in bar,
- $CE$ is a constant for erosional flow; $CE = 125$ for intermittent service and $CE = 100$ for continuous service
- $v_{\max}$ is gas velocity in m/s

In order to respect noise limitation, gas velocity in the pipe should be limited to 18 to 25 m/s.

Cavern performance is a matter of cavern thermodynamic behavior. Cavern temperature changes during a withdrawal period influence cavern pressure evolution and therefore the maximum sustainable gas flow rate. Faster and larger heat exchange is between cavern and surrounding rock, higher cavern performance.

When the withdrawal gas temperature is low enough, hydrate formation in the pipe is likely. The hydrate formation temperature limit depends on gas pressure and gas water content. Sometimes at the end of withdrawal periods, gas hydrate inhibitors are injected into the gas line before gas treatment.

**Geotechnical constraints**

High gas flow rate operations can lead to large cavern temperature changes. Large temperature variation at the cavern wall generates large thermally–induced stresses in rock salt (Brouard et al., 2011). These stresses may result in salt damage or cracking.

Besides this thermal effect, quick cycling implies high pressure change rates in the cavern and possibly severe mechanical effects as regards salt fatigue behavior or time–dependent stress distribution (refer to high cycling SMRI project which aims to enlighten these topics).

Rock salt behavior under fast thermo–mechanical cycling is not yet fully understood. Reviewing the literature, one can find the three following criteria commonly used to assess cavern stability:

❖ ***No–tension criterion***

Although salt can sustain moderate tensile stresses (salt tensile strength is limited to 1.5 – 2 MPa), it behaves brittlely under tension load. Therefore neglecting salt tensile strength is on the safe side.

Tensile stresses can result from over–pressurization of the cavern or from a thermal shock due to severe gas cooling during a production period. When roof span is too large, roof sagging is another possible reason for the occurrence of tensile stresses.

❖ ***Creep–strain criterion***

The cumulated creep strain in the rock salt must not exceed a given limit in the long term. As far as cavern design is concerned, to limit the creep strain at the salt pillar in the range of 5 % to 10% is recommended.

❖ ***The dilation/damage criterion***

It is now widely accepted that rock dilation, i.e. an increase in rock volume when it is submitted to high deviatoric stresses, is a relevant indicator of damage. Onset of dilation is predicted by a stress criterion. Two main dilation criteria can be considered. They correspond to a linear and non–linear relationship, respectively, between the second invariant of the deviatoric stress tensor and the first invariant of the stress tensor:

$$\eta = \frac{\sqrt{J_2}}{aI_1 + b} \qquad \text{(Linear damage criterion)}$$

$$\eta = \sqrt{J_2} \times \frac{\sqrt{3}\cos\theta - D_2 \sin\theta}{T_0 + D_1 \left( \frac{|I_1|}{\sigma_0} \right)^n} \qquad \text{(Non–linear damage criterion, DeVries et al., 2005)}$$

where $\theta$ is the Lode angle ($\theta = +30°$ for triaxial compression and $\theta = -30°$ for triaxial extension) ; $I_1$ is the first invariant of the stress tensor and $J_2$ is the second invariant of the deviatoric stress tensor ; $\eta$ is called the *dilation index*, $\eta \geq 1$ corresponds to a dilated state.

In the LOCAS software a Factor of Safety ($FOS$) is considered, it has the same definition as given in DeVries (2005):

$$FOS = 1/\eta \qquad (2)$$

According to this definition, dilatancy occurs when $FOS < 1$.

**Cavern loading**

Cavern stability under the second gas operation mode (seasonal micro–cycling) was compared to a purely seasonal cycling. Cavern pressure history for these two scenarios is presented here below.

Maximum and minimum cavern pressures are respectively $P_{max} = 207$ bars (3000 psi) and $P_{min} = 60$ bars (870 psi) for a 1200-m to 1400-m deep cavern.

Case #1 – Purely seasonal scenario (Figure 1)

This scenario consists of a purely seasonal cycling between $P_{max}$ and $P_{min}$ including the following stages:

- Withdrawal from $P_{max}$ to $P_{min}$ for 70 days (pressure decrease rate: 2.1 bars/day).
- Stand–by stage at $P_{min}$ for 90 days.
- Injection from $P_{min}$ to $P_{max}$ for 70 days (pressure increase rate: 2.1 bars/day).

- Stand–by stage at $P_{\max}$ for 135 days.

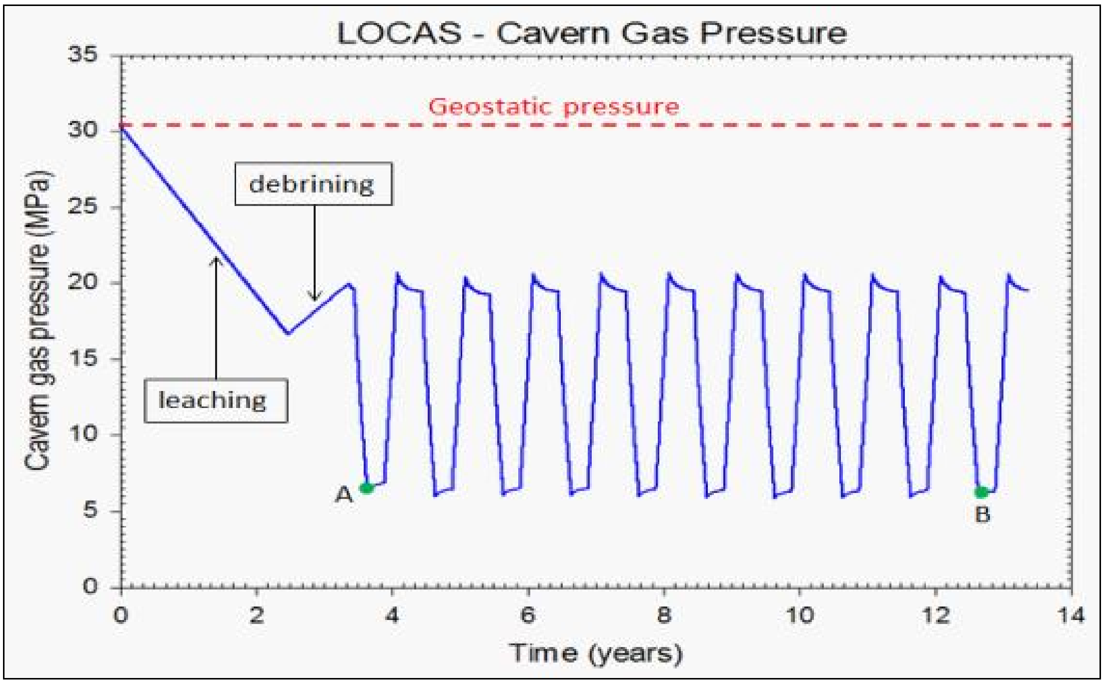


**Figure 1 – Case #1 – Cavern average pressure evolution in a purely seasonal scenario.**

<u>Case #2 – Seasonal micro–cycling scenario</u> (Figure 2)

This scenario consists of daily injections/withdrawals according to the global seasonal trend described above with the same pressure limits. The pressure history in this scenario is presented in Figure 2. Due to surface facilities limitation, at maximum pressure ($P_{\max}$) the maximum gas flow rate varies between $4.8 \times 10^6 \ \mathrm{Nm}^3/\mathrm{day}$ and the maximum pressure rate is 7 bars/12 hours. At minimum pressure ($P_{\min}$), the maximum flow rate is $4 \times 10^6 \ \mathrm{Nm}^3/\mathrm{day}$ because of gas velocity limitation of 25 m/s, and the maximum pressure rate is 3 bars/12 hours.

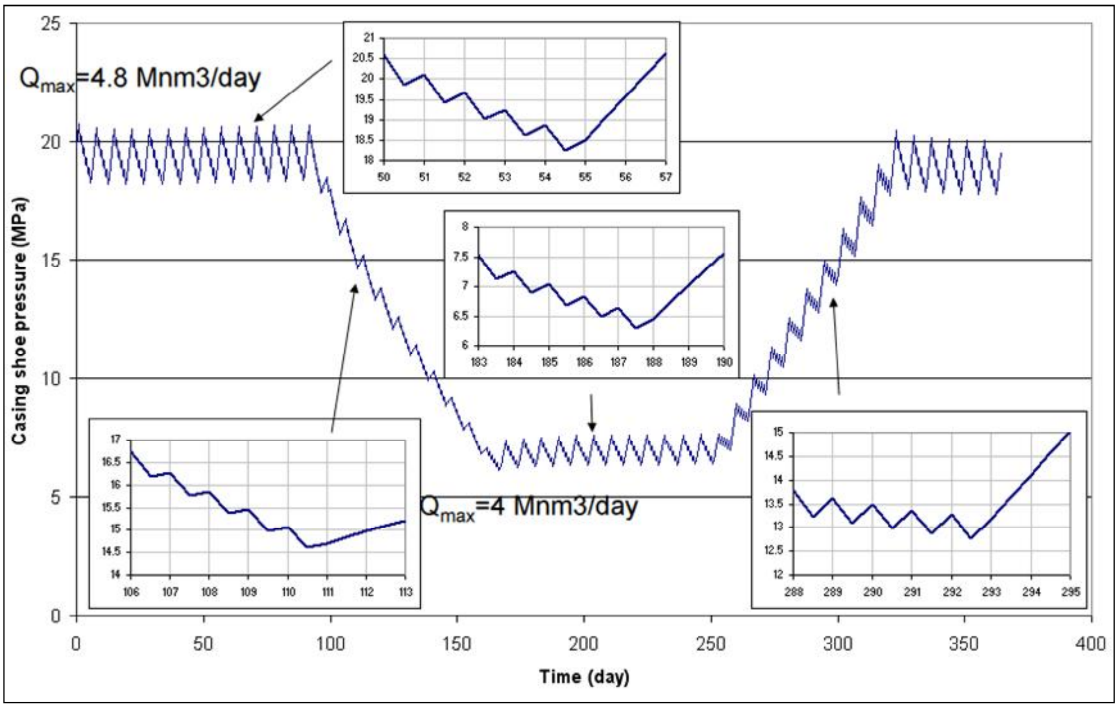


**Figure 2 – Case #2 – Casing shoe pressure evolution in a seasonal micro–cycling scenario.**

**Numerical modeling**

These two scenarios were modeled considering a cylindrical cavern whose main characteristics are as follows:

- Cavern mean depth: 1400 m (4600 ft)
- Cavern diameter: 70 m (230 ft)
- Cavern height: 400 m (1312 ft)
- Gas production tube: 9–5/8"
- Cavern excavated volume: 1,482,000 $m^3$ (9.3 MMbbls)

Two different approaches for numerical computations where considered:

1. SCTS + ABAQUS
2. LOCAS only

**Thermo–dynamical computations**

Cavern thermodynamic analysis has been carried out with the following parameters:

- Natural salt temperature at cavern mean depth: 58°C (136°F)
- Gas entry temperature: 30°C (86°F)
- Cavern leaching duration: 900 days
- Cavern debrining duration: 11 months
- Gas operation duration: 35 years

- In the first approach SCTS software (GTI, 2004) was used to calculate the evolution of cavern gas temperature for the given pressure scenarios. Gas inflows/outflows had to be fitted to get the required cavern pressure evolutions. In the SCTS model cavern shape is considered spherical and there is a radiative heat transfer at cavern wall. A free volume of 685,000 $m^3$ was taken into account and a cavern volume to area ratio of 12 was considered. In this approach, it is supposed that salt in the vicinity of the cavern wall is cooled by cavern leaching.

- In the second approach, LOCAS considered the excavated volume (1,482,000 $m^3$) for the thermo–dynamical computations and heat flux from rock mass is calculated from the actual shape of the cavern considering a continuous temperature at cavern wall. Cavern mesh is shown on Figure 2; the maximum size of mesh elements at cavern wall is 10 cm (0.3 ft), this small size is required in order to calculate accurately temperature distribution in the vicinity of cavern wall (Brouard et al., 2011). In this approach gas temperature is assumed to be equal to geothermal temperature (58°C) at the end of debrining. Salt in the vicinity of the cavern is not assumed to be cooled by cavern leaching.

In the first approach cavern temperature evolution calculated using SCTS was applied at cavern wall in the ABAQUS finite elements software. In the second approach the coupled thermo–mechanical computations are performed by LOCAS.

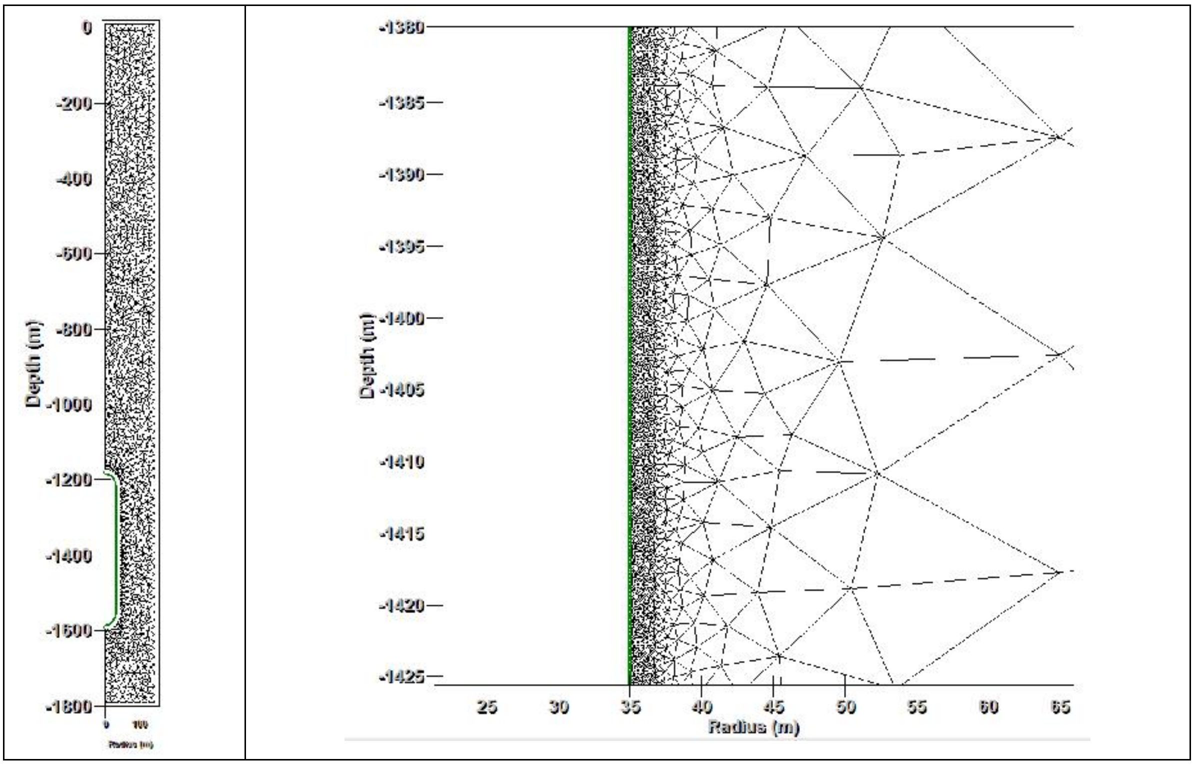


**Figure 3 – Mesh used in LOCAS computations.**

**Mechanical computations**

Natural stress condition was considered isotropic with a 29.5 MPa (4280 psi) geostatic stress at cavern mid–depth. Horizontal displacements were blocked at 147 m from cavern axis to take into account neighboring caverns.

***Constitutive law***

The Lemaitre–Menzel–Schreiner constitutive law was used to describe the salt viscoplastic behavior. In its simplified uniaxial form (used when fitting creep tests results), the strain–stress Lemaitre creep law can be expressed as:

$$\varepsilon_t = \varepsilon_e + \varepsilon_{vp} = \sigma/E + \varepsilon_{vp} \tag{3}$$

Where $\varepsilon_t$ is the total strain, $\varepsilon_e$ is the elastic strain, $\varepsilon_{vp}$ is the viscoplastic strain, $\sigma$ is the applied deviatoric stress, and $E$ is the Young modulus. The viscoplastic strain (μm/m) can expressed as:

$$\varepsilon_{vp} = \left(\frac{\sigma}{K}\right)^{\beta} \exp\left(-\frac{Q}{R}\left[\frac{1}{T} - \frac{1}{T_r}\right]\right) \times t^{\alpha} \tag{4}$$

Where $(\alpha, \beta, K)$ are Lemaitre parameters, $t$ is time in days, $T$ is salt temperature in Kelvins, $T_r$ is a reference temperature, and Q/R is the Arrhenius coefficient. The Lemaitre parameters considered in this study are as follows:

$$\alpha = 0.3 \quad K = 0.49 \text{ MPa at } T_r = 58°\text{C}$$
$$\beta = 2.2 \quad Q/R = 3000 \text{ K}$$

The Vouille's index is sometimes used for comparing the creep potentials of different salt formations, it is defined as the cumulated axial viscoplastic strain experienced by a sample which has been submitted to a 10–MPa deviatoric stress for one year at the reference temperature. The Vouille's index for the salt formation considered in this study is about 0.45% at the reference temperature, a figure associated to a low creep prone salt.

***Dilatation criterion***

The values of the parameters used for the DeVries dilation criterion are as follows:

$$n = 0.75 \qquad D_1 = 1.15 \qquad D_2 = 0.5$$
$$T_0 = 1.5 \text{ MPa} \quad \sigma_0 = 1 \text{ MPa}$$

**ABAQUS simulations results**

ABAQUS results regarding onset of salt tensile stresses and dilation index $\eta$ value were analyzed. Computations were performed for a 35–year long period of gas operation. The maximum principal stresses $\sigma_{max}$ (less compressive) at first and last minimum pressure ($P_{min}$) gas operation period, during year 1 and year 35, for Case #1 and Case #2 are shown in Figure 4 and 5. In both cases, stresses remain compressive at cavern wall. It can be observed that, at the end of leaching and during the first (year 1) and last (year 35) period during which the pressure is minimum, the least compressive stress at cavern wall is the normal stress (or cavern gas pressure) which is a linear function of depth. During the last minimum–pressure period (after 35 years of operation), the least compressive stress is a tangential stress –a switch which is currently observed in any cavern operated during a long period of time and can be associated to a slow decrease in the average deviatoric stress originating in salt creep.

The area most vulnerable to tensile failure is the cavern roof. The maximum principal stress at cavern roof reach –2 MPa in the case 1 (purely seasonal scenario) and –6 MPa in the case 2 (seasonal micro–cycling) at $P_{min}$ after 35 years of gas operation.

The dilation state is represented by the dilation index. The non–linear dilation index at the first and last minimum gas pressure is checked (Figure 6 and Figure 7).

The maximum value of this index along the cavern wall ranges between 0.8 – 1.1 for case #1 and #2. The index decreases slowly in the pillar to reach a value equal to 0.2 at mid–pillar in both cases.

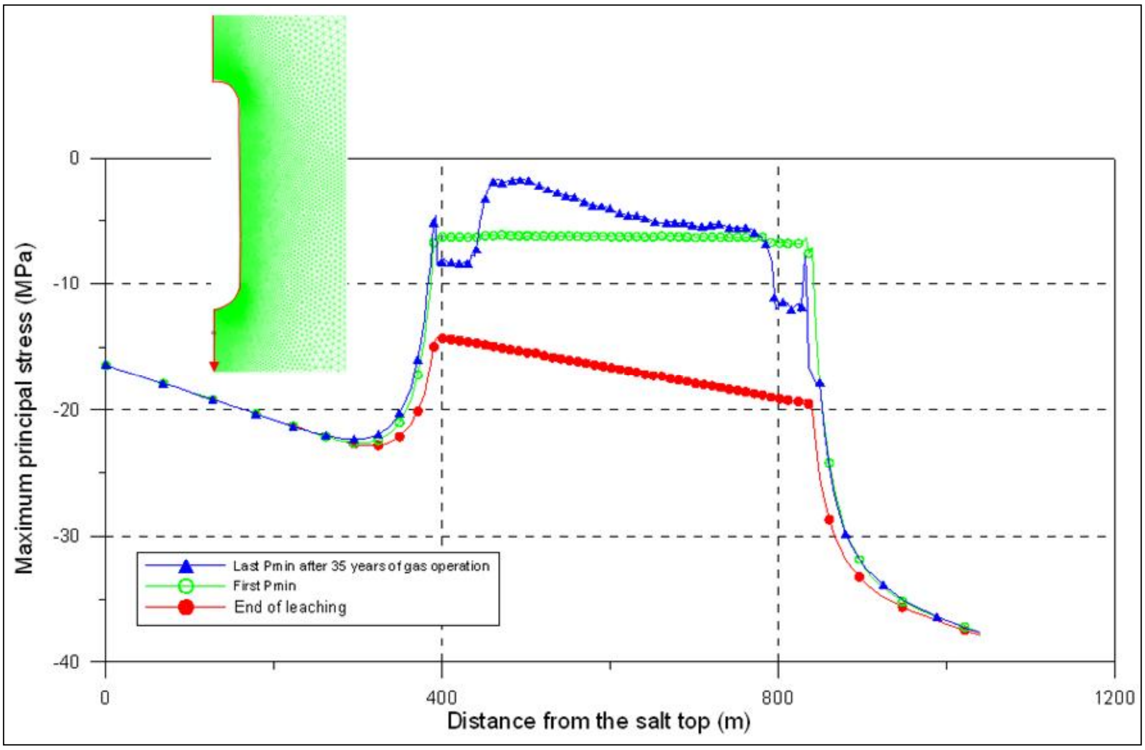


**Figure 4 – Case #1 – Purely seasonal scenario – Maximum principal stress (least compressive) along a vertical profile [ABAQUS].**

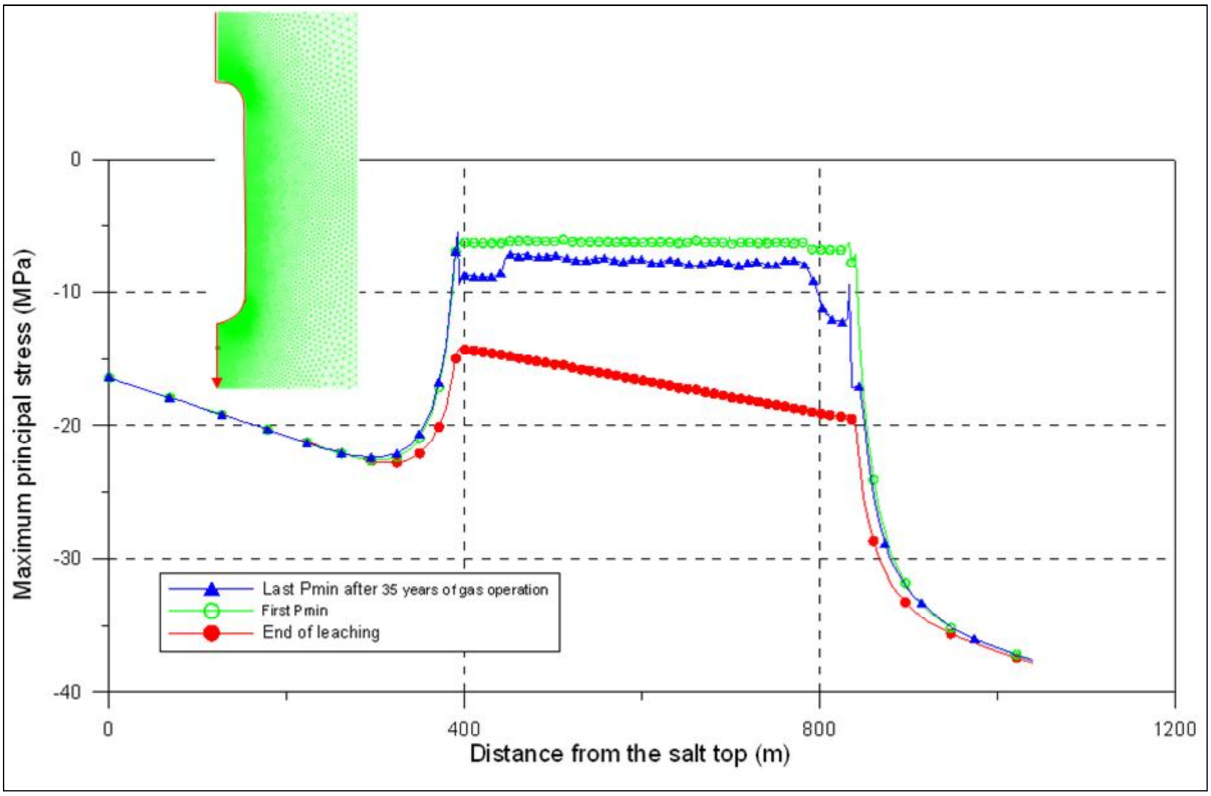


**Figure 5 – Case #2 – Seasonal micro–cycling scenario – Maximum principal stress (least compressive) along a vertical profile [ABAQUS].**

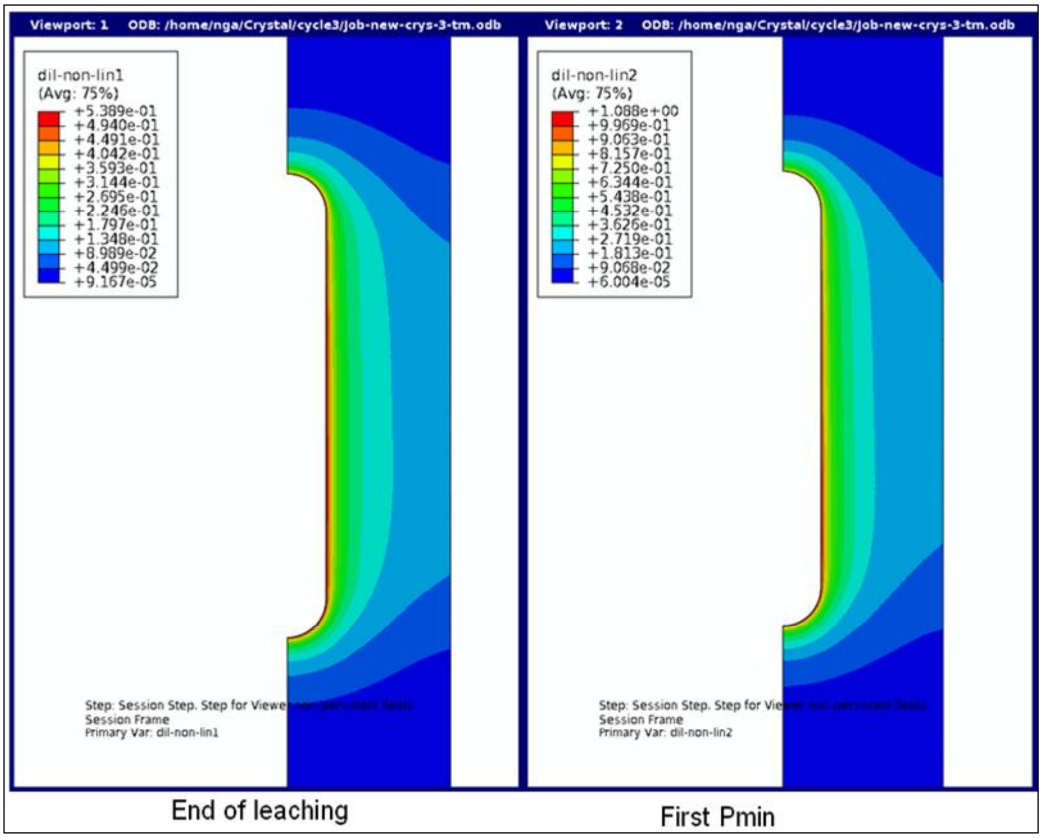


**Figure 6 - Case #1 – Purely seasonal scenario – Dilation index [ABAQUS].**

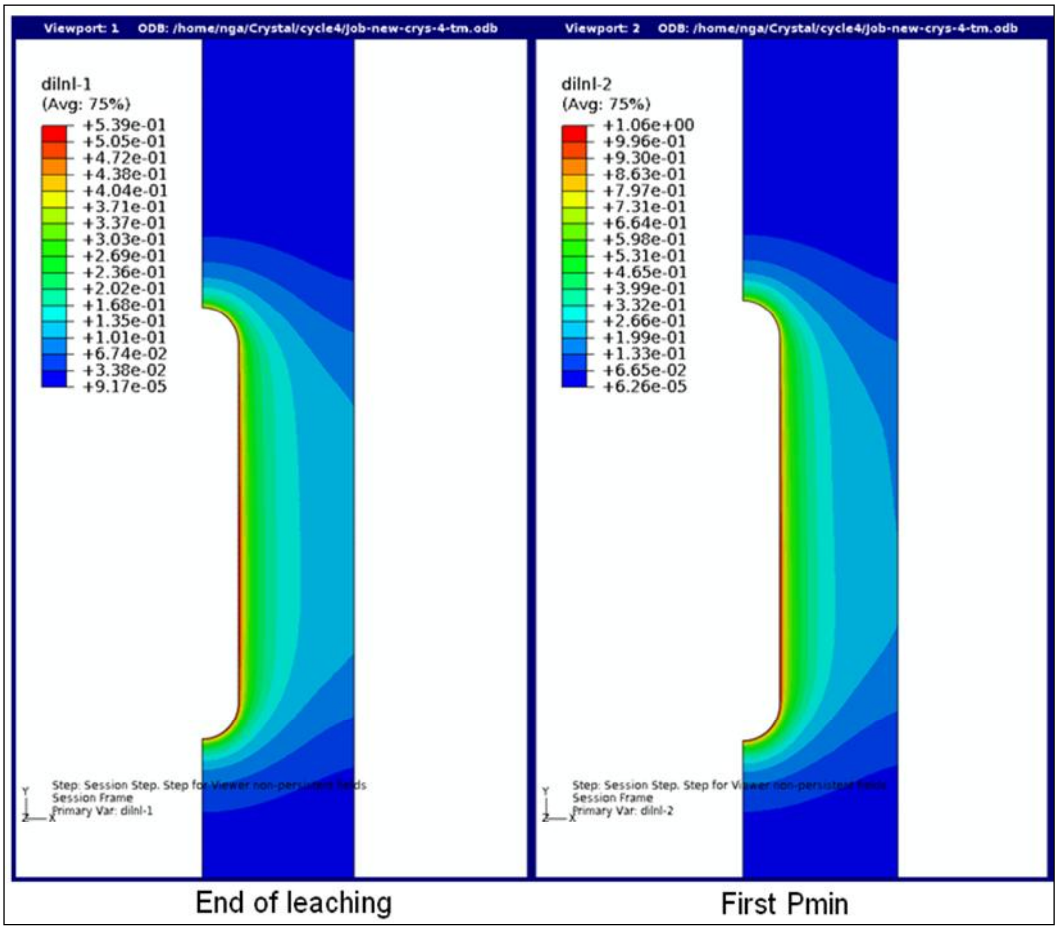


**Figure 7 – Case #2 – Seasonal micro–cycling scenario – Dilation index [ABAQUS].**

**LOCAS simulations results**

Figure 8 and Figure 9 show cavern temperature evolutions as computed by LOCAS for both scenarios. During each cycle, temperature drops abruptly during gas withdrawal and slowly increases when gas pressure is kept minimum (heat flux from the rock mass is given time enough to warm cavern gas). Conversely temperature swiftly increases when gas is injected in the cavern and slowly decreases when gas pressure is kept maximal. Steady-state heat flux from the rock mass is small (Figure 10); however, following any rapid temperature increase of decrease, transient heat flux is as large as several MW.

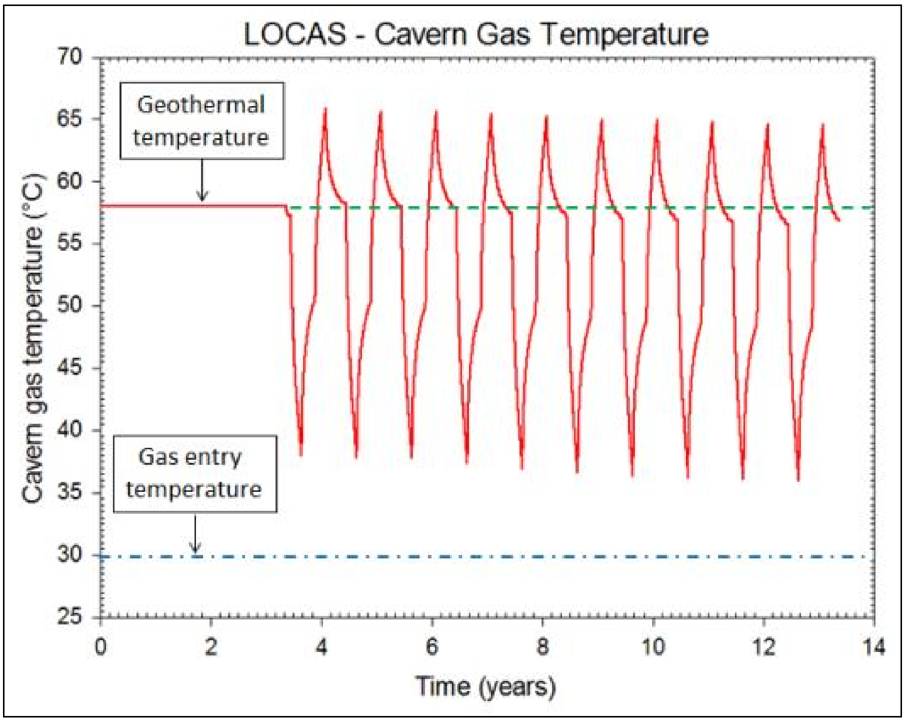


**Figure 8 – Case #1 – Purely seasonal scenario – Cavern temperature evolution [LOCAS].**

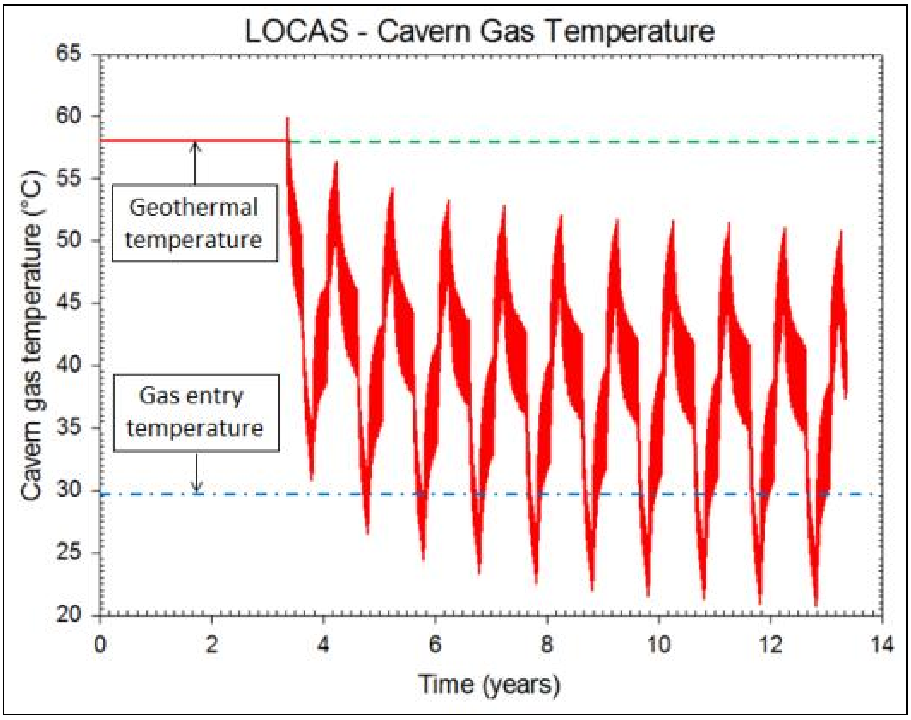


**Figure 9 – Case #2 – Seasonal micro–cycling scenario – Cavern temperature evolution [LOCAS].**

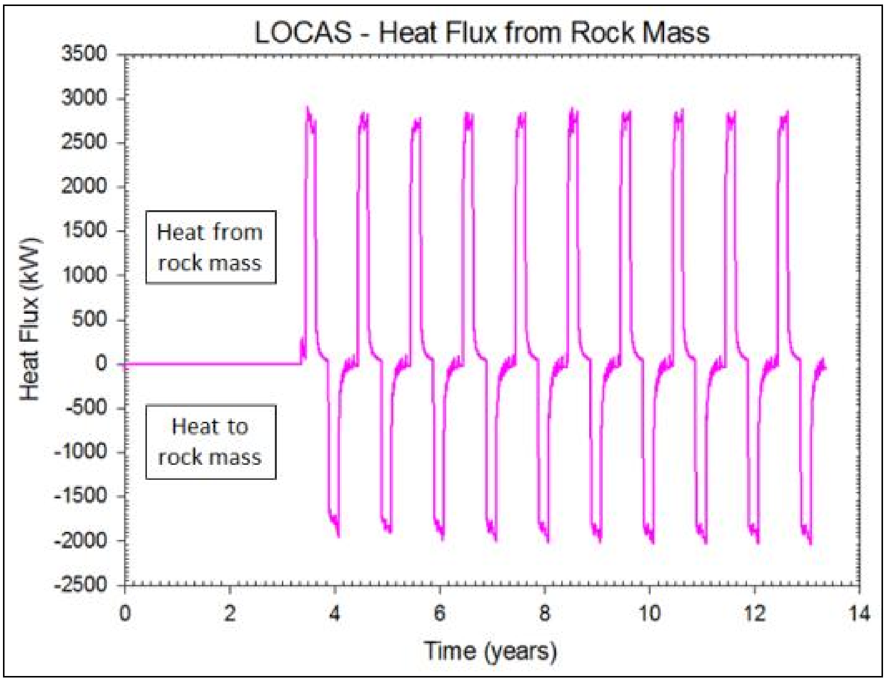


**Figure 10 – Case #1 – Purely seasonal scenario – Evolution of heat flux from rock mass [LOCAS]**

Figure 11 is a contour plot of the maximum principal stress (least compressive) at the first minimum pressure in Case #1. No tensile stresses appear; the maximum stress is -6.2 MPa (compressive). Figure 12 is the same plot for Case #2. Stresses are larger in Case #2 than in Case #1 but there are still compressive; the maximum stress is -3.7 MPa.

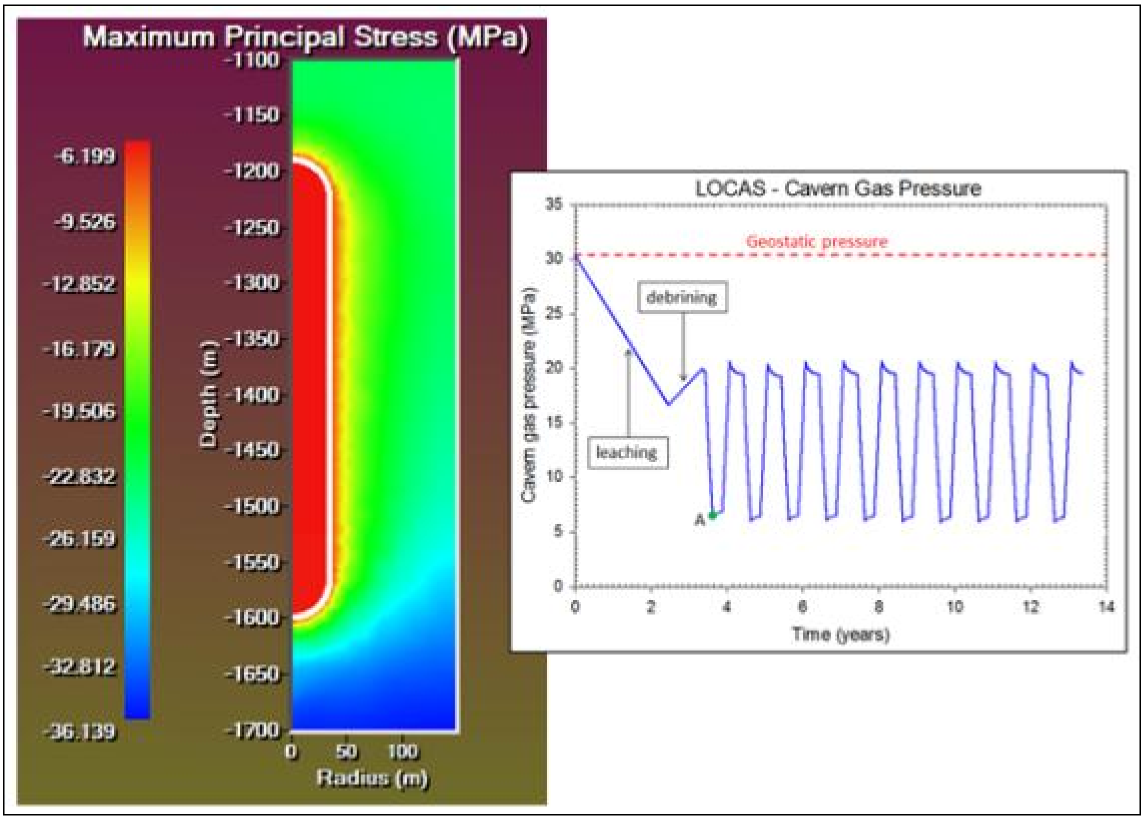


**Figure 11 – Case #1 – Maximum principal stress (least compressive) in the vicinity of the cavern at first minimum pressure (point A) [LOCAS].**

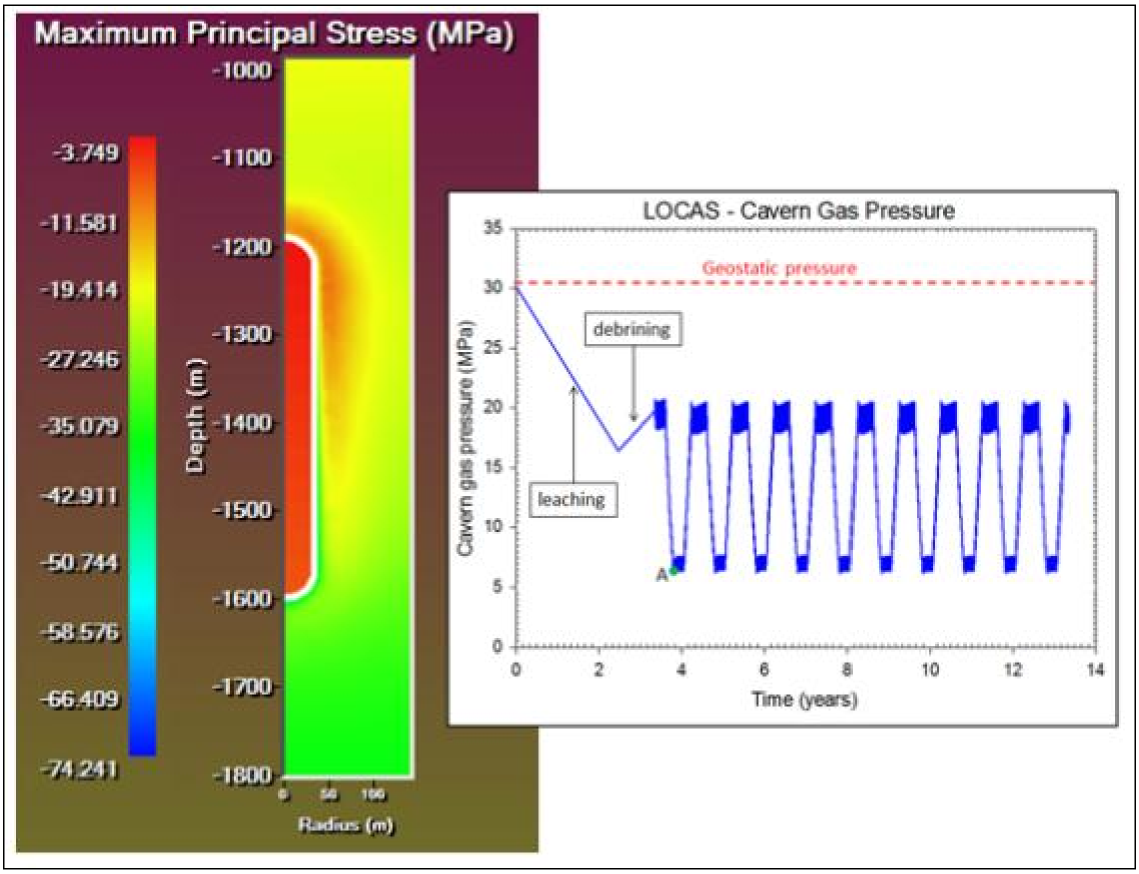


**Figure 12 – Case #2 – Maximum principal stress (least compressive) in the vicinity of the cavern at first minimum pressure (point A) [LOCAS].**

Figure 13 shows a contour plot of DeVries dilation criterion at the first minimum pressure for Case #1. No dilation occurs, the minimum factor of safety is FOS=1.16.

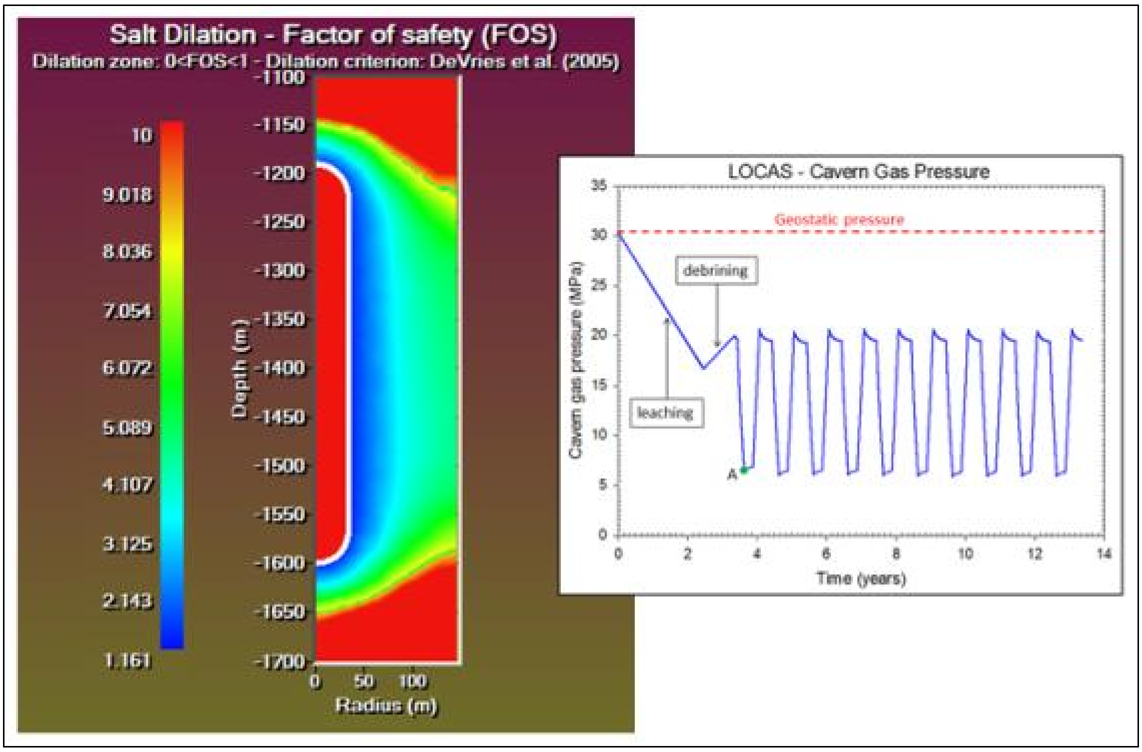


**Figure 13 – Case #1 – DeVries dilation criterion at first minimum pressure (point A) [LOCAS].**

Figure 14 shows a contour plot of DeVries dilation criterion at the first minimum pressure for Case #2. No dilation occurs and the minimum factor of safety is larger than in Case #1, i.e. safer. Figure 16 shows the same dilation criterion for the first minimum pressure of 10th cycle (point B) for Case #2; the minimum factor of safety (FOS=2.7) is even greater than for the first cycle.

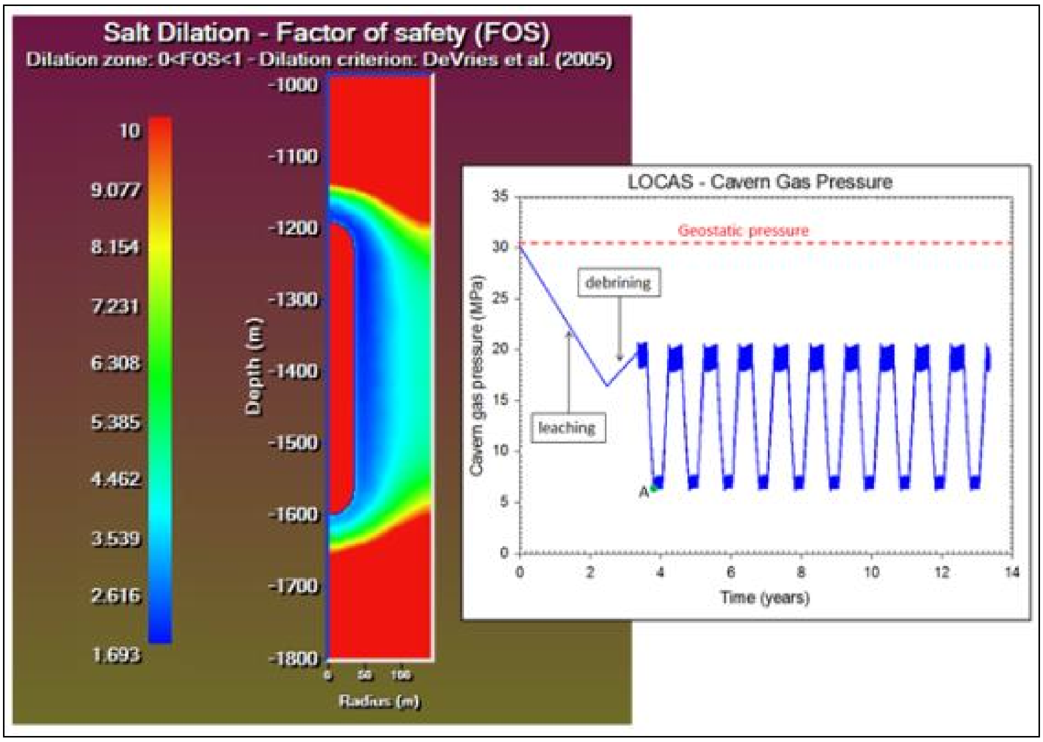


**Figure 14 – Case #2 – DeVries dilation criterion at first minimum pressure (point A) [LOCAS].**

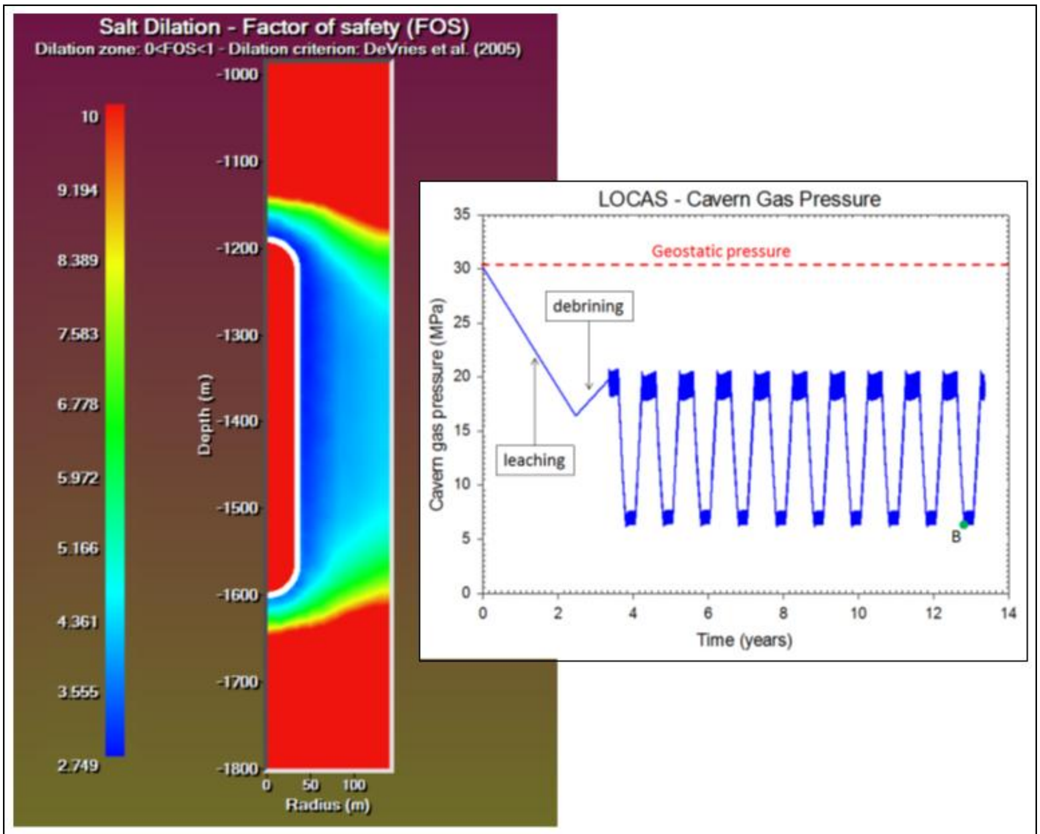


**Figure 15 – Case #2 – DeVries dilation criterion at 10th minimum pressure (point B) [LOCAS].**

On Figure 16 and Figure 17, for the two selected scenarios, the path followed by the state of stress in the invariants plane $\left(-I_1/3, \sqrt{3J_2}\right)$ is represented together with four dilation criteria, the Ratigan, Spiers, DeVries (extension) and DeVries (compression) criteria. The state of stress is computed at the cavern wall, at a 1463–m depth, a location which is representative of the mechanical behavior of the cavern main body. Four different colors are used, depending whether the state of stress is tensile, dilated, both tensile and dilated, or "normal" (i.e., no criterion is reached). Note that during the two considered scenarios, the state of stress is "normal" except during short period of times in Scenario 2, when the considered point at cavern wall experiences dilatancy.

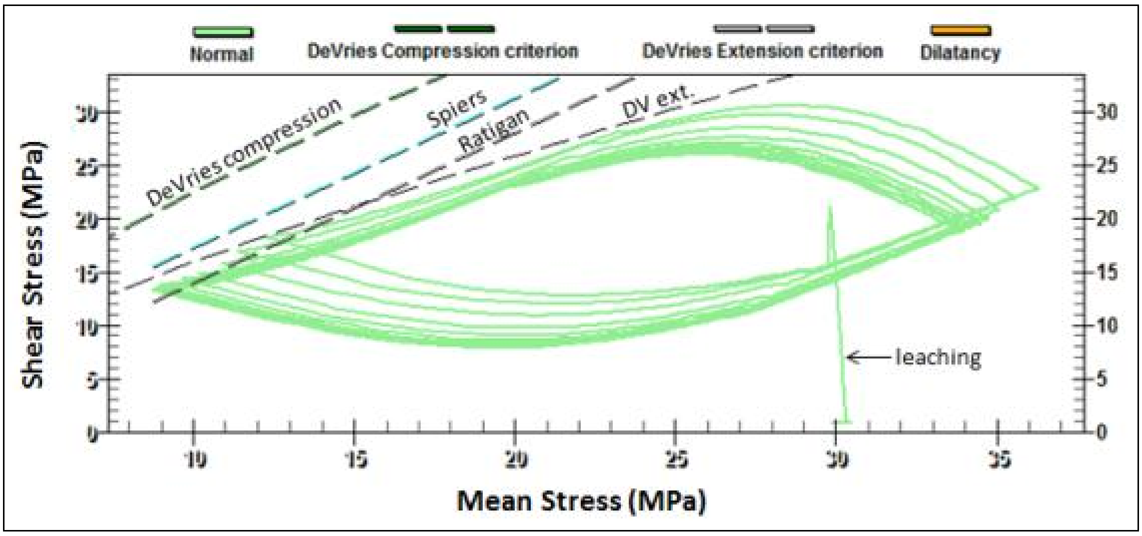


**Figure 16 – Case #1 – Purely seasonal scenario – Evolution of the state of stress in the invariant plane [LOCAS].**

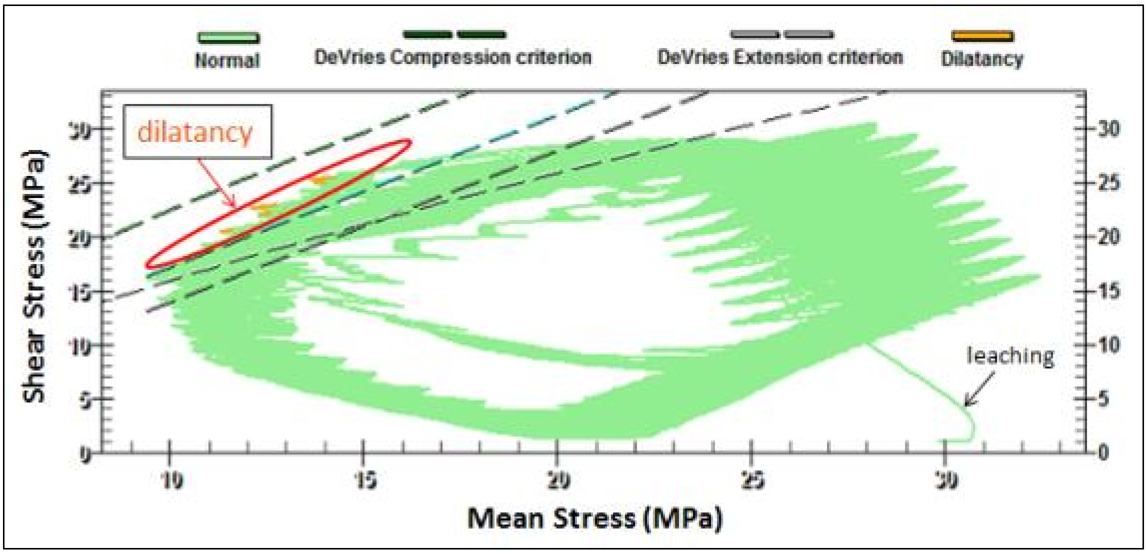


**Figure 17 – Case #2 – Seasonal micro–cycling scenario – Evolution of the state of stress in the invariant plane [LOCAS].**

**Optimization of gas storage performance using SCTS**

In order to increase the storage performance, a seasonal multi–cycle operation mode can be optimized to produce higher flow rates during withdrawal periods and to make available higher working gas volume during an annual cycle.

The optimization of the seasonal micro–cycling operation consists in increasing the daily production gas flow rates when all the operational and geotechnical constraints are considered.

As shown in the Figure 18 and Figure 19 a typical seasonal micro–cycling operation consists of the following stages:

a) Withdrawal stage: the working gas is extracted for a couple of weeks. A weekly cycle consists of high production rate and low injection rate during daily operations.
b) Stand–by stage at low pressure: the gas inventory keeps constant during weekly cycles with some daily production /injection operations of the same order of magnitude.
c) Injection stage: the working gas is injected into the cavern through couple of weekly cycles. Each weekly cycle consists of low production /high injection daily operations.
d) Stand–by stage at high pressure: the gas inventory increases very slowly to reach the maximum inventory. Daily cycles in this stage are designed to inject a little more than what is produced weekly.

The advantage of such a multi–cycling operation is that it follows at the same time the seasonal trend (high production in winter and storage filling in summer), the weekly trend (high production demand on working days and high injection on weekends) and the daily trend (production at working hours and injection at night).

In this study, several thermodynamic simulations were performed with SCTS to optimize such multi–cycling operation for higher flow rates and larger working gas by taking into account the following limitations:

- Cavern pressure rate limited to 10 bars/day during withdrawal (geotechnical issue).
- Withdrawal gas temperature warmer than the hydrate formation temperature.
- Gas velocity limited to 25 m/s (tube erosion).
- Gas flow rate limited by surface facilities

.
The following optimizations were inferred from SCTS thermodynamic simulations (Figure 20):

- The maximum gas flow rate (MGFR) is determined by cavern pressure rate limitation at the beginning of the withdrawal stage at high pressure. The other constraints on the MGFR are the total stage duration and the cavern temperature drop. During the withdrawal stage, the MGFR has to be reduced progressively to respect the hydrate formation and gas velocity limitations especially at the end of the withdrawal stage.
- During the stand–by stage at low pressure, the MGFR can be built up along with the cavern temperature increase. At the end of this stage, gas velocity is the most demanding limitation.
- During the injection stage, pressure builds up, and the MGFR can increase until the maximum pressure is reached.
- The MGFR is kept constant during the stand–by stage at high pressure.

***Example of an optimized cavern operation***

The cycle presented here corresponds to a total gas inventory of $76\times10^6\ \mathrm{Nm}^3$ and a working gas volume of $49\times10^6\ \mathrm{Nm}^3$. The annual gas production volume in this case reaches $532\times10^6\ \mathrm{Nm}^3$. The MGFR at high pressure is about $4.3\times10^6\ \mathrm{Nm}^3/\mathrm{day}$.

The modeled cavern has the following characteristics:

- Cavern physical volume : 400,000 $m^3$ (2.5 MMbbls)
- Cavern maximum and minimum pressure are 185 bars (2683 psi) and 60 bars (870 psi).

- Casing shoe depth: 1000 m (3280 ft)

The cavern pressure and temperature evolution corresponding to the seasonal micro–cycling presented above are illustrated in Figure 21 and Figure 22.

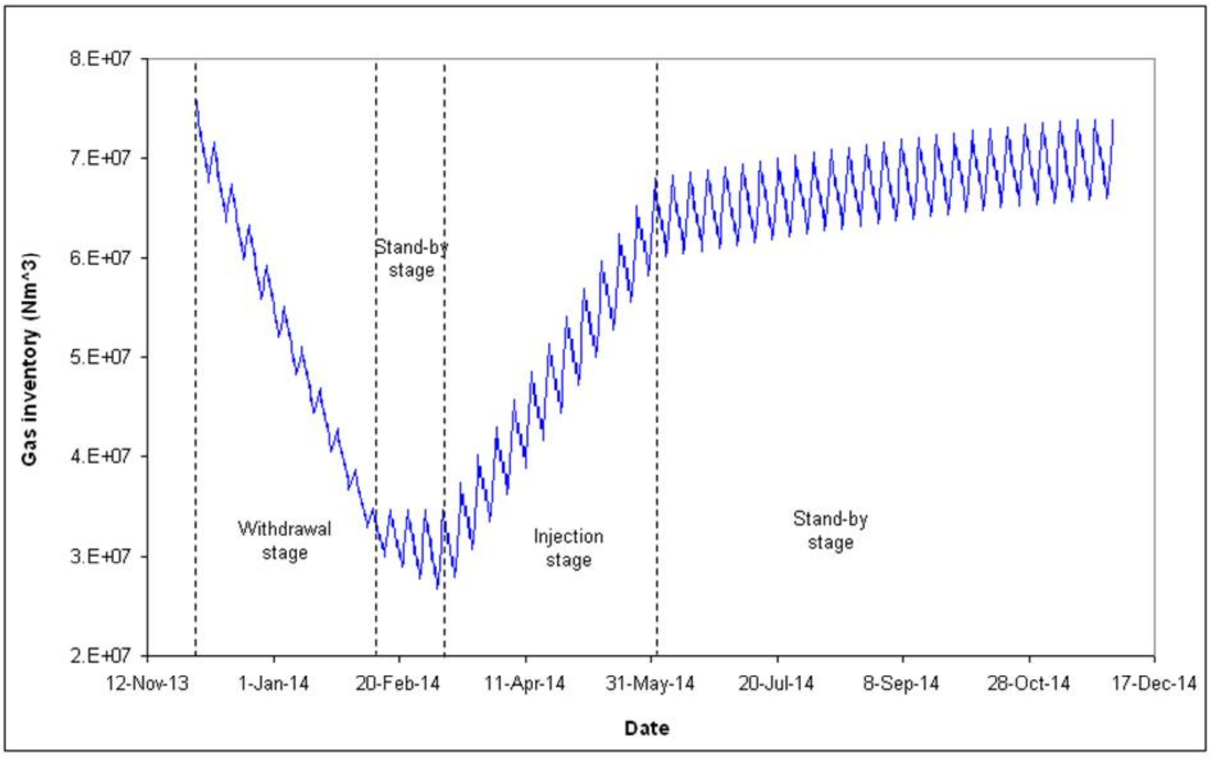


**Figure 18 – Typical seasonal micro–cycling operation.**

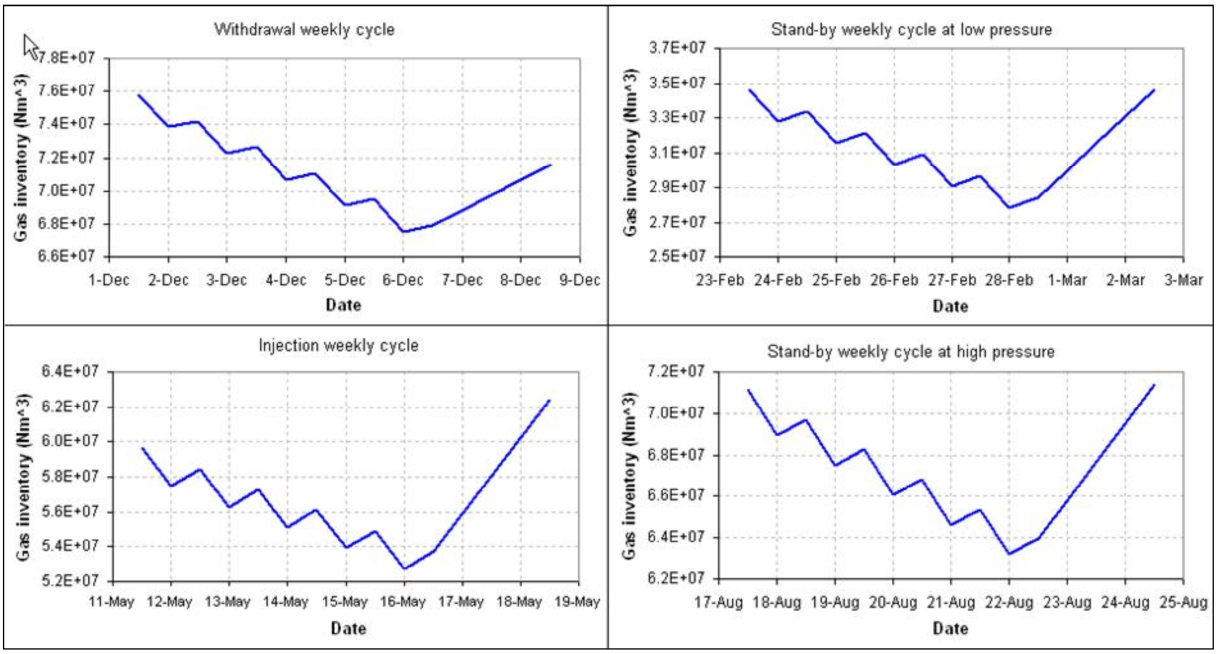


**Figure 19 – Weekly pressure variations.**

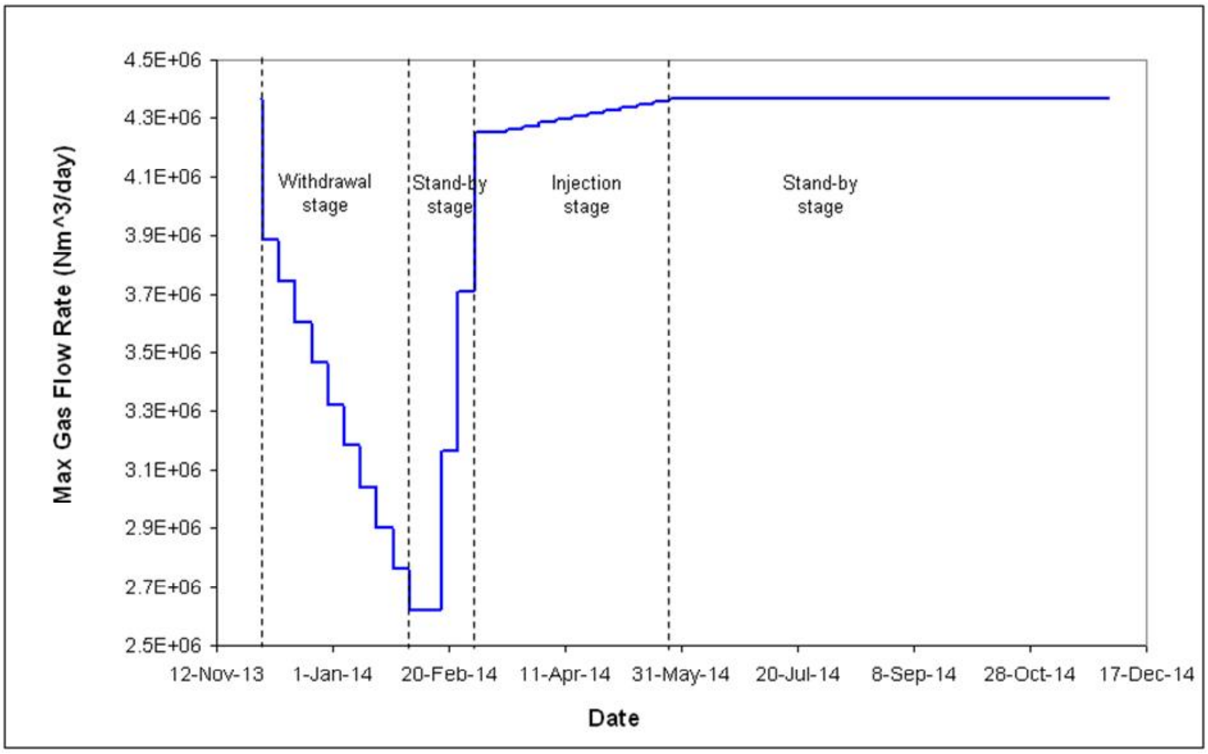


**Figure 20 – Optimization of the maximum gas flow rate.**

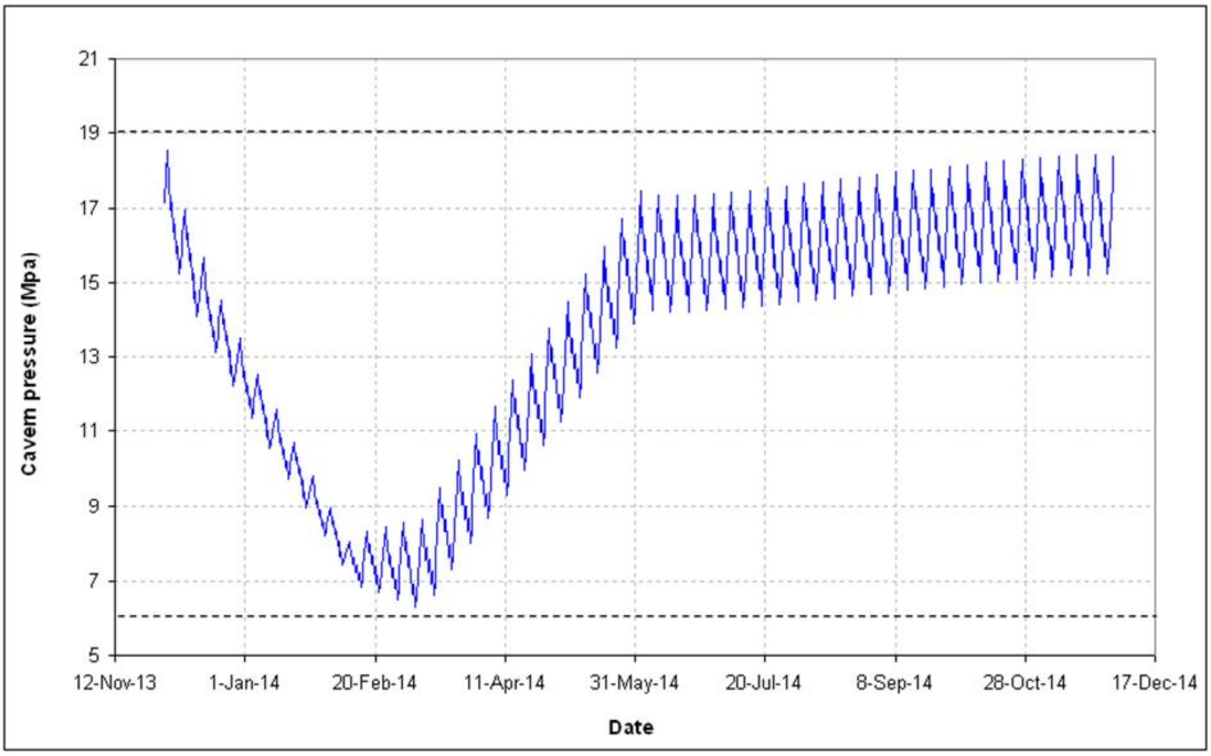


**Figure 21 – Cavern pressure variation during one annual cycle.**

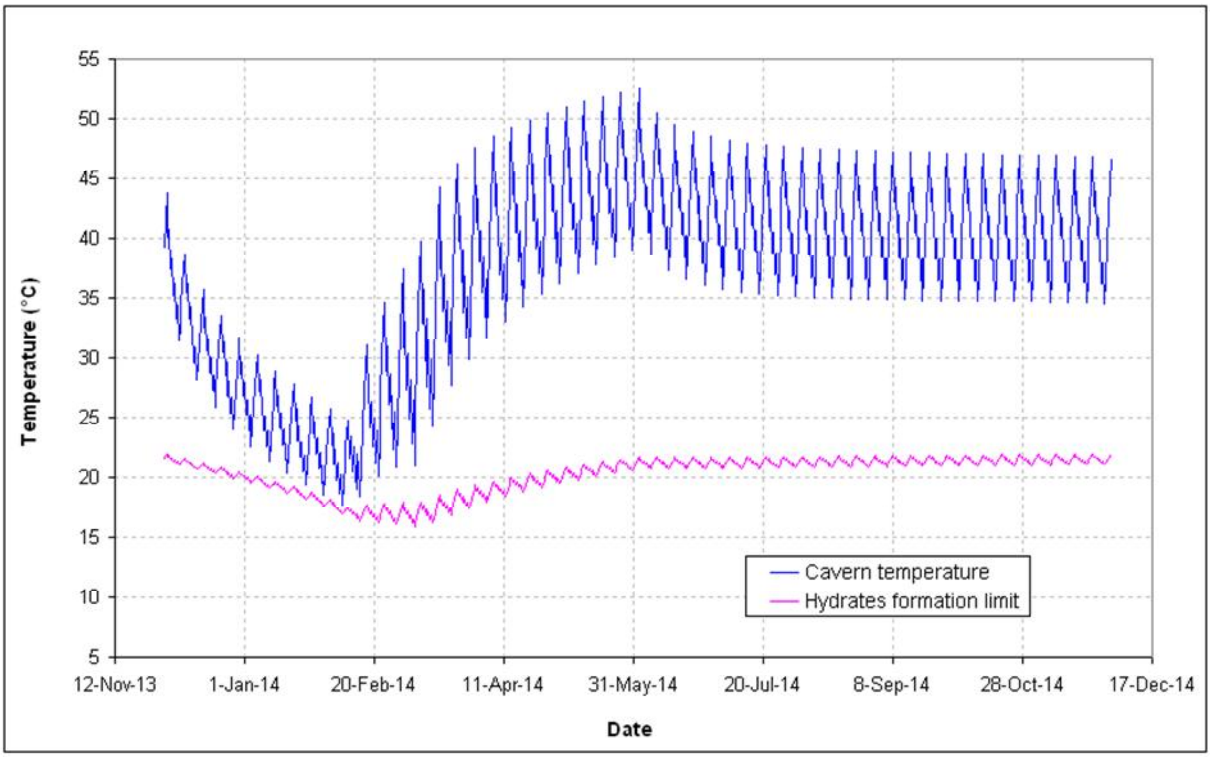


**Figure 22 – Cavern temperature variation during one annual cycle.**

### Conclusions

Rock mechanical calculations performed with two different numerical simulators (ABAQUS+SCTS and LOCAS) lead to similar conclusions with regard to the effects of the seasonal and micro–cycling operation modes.

The computations have proved that a seasonal micro–cycling operation mode is not more critical than a purely seasonal operation mode with the same maximum and minimum pressure. The advantage of the former cycle is to provide more flexibility and a larger working volume during operation.

Regarding the no–tension criterion, ABAQUS computations seem to show that the seasonal micro–cycling triggers less thermal induced stresses than the pure seasonal operations; on the contrary LOCAS computations show that the stresses are a bit less compressive in the micro-cycling scenario. Both ABAQUS and LOCAS computation predict that the stresses remain compressive.

The salt dilation predicted by the numerical calculations is similar for the both scenarios.

### References

Brouard B., Frangi A. and Bérest P. *Mechanical stability of a cavern submitted to high–frequency cycles*. Proc. SMRI Spring Meeting, Galveston (2011).

DeVries K.L., Callahan G.D. and Mellegard K.D.*Numerical Simulations of Natural Gas Storage Caverns in Bedded Sal*t. ARMA/USRMS 05–734, Proceedings, 40$^{th}$ U.S. Symposium on Rock Mechanics, University of Alaska Anchorage, Anchorage, AK, June 25–29, G. Chen, S. Huang, W. Zhou, and J. Tinucci Eds. (2005).

American Petroleum Institute – *API 14E Recommended Practice for Design and Installation of Offshore Products Platform Piping Systems* (1991).

Gas Technology Institute – Salt Cavern Thermal Simulator – version 2.0 User's Manual (2004).